J. Fluid Mech. (1981), *vol.* 104, *pp.* 387–405
Printed in Great Britain

A visual study of turbulent spots

By A. E. PERRY, T. T. LIM AND E. W. TEH

Department of Mechanical Engineering, University of Melbourne,
Parkville, Victoria 3052, Australia

(Received 12 September 1979 and in revised form 1 August 1980)

From the results of a flow visualization experiment, certain physical characteristics of a turbulent spot are suggested by the authors. The spot was artificially initiated at a point by a small intermittent wall jet. The authors also carried out experiments behind vibrating trip wires and observed the 'signatures' or 'footprints' of the Λ-shaped vortices seen by other workers. The fact that these 'signatures' are also observed in a turbulent spot leads one to suspect that these spots consist essentially of an array of Λ-shaped vortices. The formation of the spot is subsequently described in terms of three-dimensional disturbances of the cross-stream vortex filaments.

The basic structure of the turbulent spot proposed here is similar to the suggested structure of fully developed turbulent boundary layers first put forward by Theodorsen (1955) and more recently by Bandyopadhyay & Head (1979).

1. Introduction

The role which turbulent spots play in the transition process in boundary-layer shear flow has been of great interest since they were discovered by Emmons (1951). It has been suggested that turbulent spots in the laminar boundary layer (Emmons 1951; Schubauer & Klebanoff 1956) might contain certain physical properties which are common with structures in the fully developed turbulent boundary layer. This suggestion has motivated many people to study the 'anatomy' of a turbulent spot.

Recently, Coles & Barker (1975), Wygnanski, Sokolov & Friedman (1976) and Cantwell, Coles & Dimotakis (1978) suggested that a turbulent spot consists essentially of one or two large coherent eddies. The authors contend that this is true only in the phase-averaged sense and believe that the 'large-eddy' structure of a spot as deduced by them is an average over a more detailed underlying structure that has 'jitter' or variance from realization to realization. The present authors are more interested in this detailed underlying structure of the spot.

An experimental investigation was therefore conducted using a boundary-layer smoke tunnel similar in design to that of M. R. Head of the University of Cambridge. Some preliminary attempts were made to artificially stimulate the transition process from trip wires and from isolated points in the flow in a purely periodic way. By the use of stroboscopic light which was synchronized with the disturbance, it was hoped to 'freeze' the process in time, in a manner similar to the procedure of Perry & Lim (1978) with coflowing jets and wakes. This 'freezing' process was only partially successful. Nevertheless some detailed features of the anatomy of a turbulent spot suggested themselves and are reported here. These proposed structures are similar to those fully developed turbulent boundary-layer structures first suggested by Theodorsen (1955)

0022-1120/81/4690-3730 $02.00

and subsequently by many other workers. Bandyopadhyay & Head (1979) have shown very convincingly by a flow-visualization technique that turbulent boundary layers consist of closely packed Λ-shaped† vortices which lean forward in the downstream direction.

2. Apparatus

The smoke tunnel is 10·4 m long, 1·2 m wide, and 0·91 m high and details are given in figure 1. The upstream end is fitted with a honeycomb followed by four wire gauze screens. There is no contraction incorporated in the tunnel.

The smoke used in the experiment was generated by a smoke generator developed by the authors. Shell Ondina 15 grade oil was evaporated to form a mist which was introduced into the tunnel through a spanwise slit 1·6 mm wide flush with the floor of the tunnel. This slit provided the outlet for the smoke, which formed a thin layer on the floor. The height of the smoke–air interface was found to be Reynolds number dependent and the operating free-stream velocity in the tunnel was within the range 0·3–3·5 m s^{-1}.

To make detailed examination of the flow structure, a transverse cross-section of the smoke was made visible by a sheet of laser light from a 5 mW He–Ne laser. As shown in figure 1, the laser beam was transformed into a plane sheet by means of a glass rod transverse to the axis of the beam. The sheet could be shifted to different streamwise positions since the laser assembly was mounted on an air-bearing sled which ran parallel to the axis of the tunnel. All phenomena were recorded by still camera shots and cine photography. The movies were examined frame by frame with a motion analysis projector.

3. Flow visualization

3.1. *Trip-wire experiments*

The investigation of the three-dimensional nature of boundary-layer instability was conducted using a vibrating trip-wire method. A stainless-steel rod 4·15 mm in diameter was placed transverse to the flow with a gap of 3 mm between the rod and the floor and 24 cm from the streamwise origin of the boundary layer. This origin is defined here as the position of the last screen. At the trip wire, the boundary layer was approximately 1 cm thick and the smoke layer was 2 mm thick. Figure 2 shows some typical patterns in the layer of smoke. The authors suspected that these patterns were the 'signatures' or 'footprints' of Λ-shaped vortices which were being stretched in the streamwise direction. Insufficient smoke was being entrained away from the boundary to make the Λ-shaped vortices visible. However, when the rod was submerged in the smoke at the wall level and the streamwise position of the rod was shifted to 96 cm from the last screen, the vortices were most visible as shown in figure 3(*a*). The boundary layer in this case was approximately 2 cm thick at the trip wire. These vortices were enhanced and made more orderly as seen in figure 3(*b*) by oscillating the rod as was commonly done for initiating a Tollmein–Schlichting type of instability – e.g. see Schubauer & Skramstad (1948), Klebanoff & Tidstrom (1959)

† Some people refer to these as hair-pin vortices, horse-shoe vortices or vortex loops. The authors are using the Λ notation of Hama & Nutant (1963).

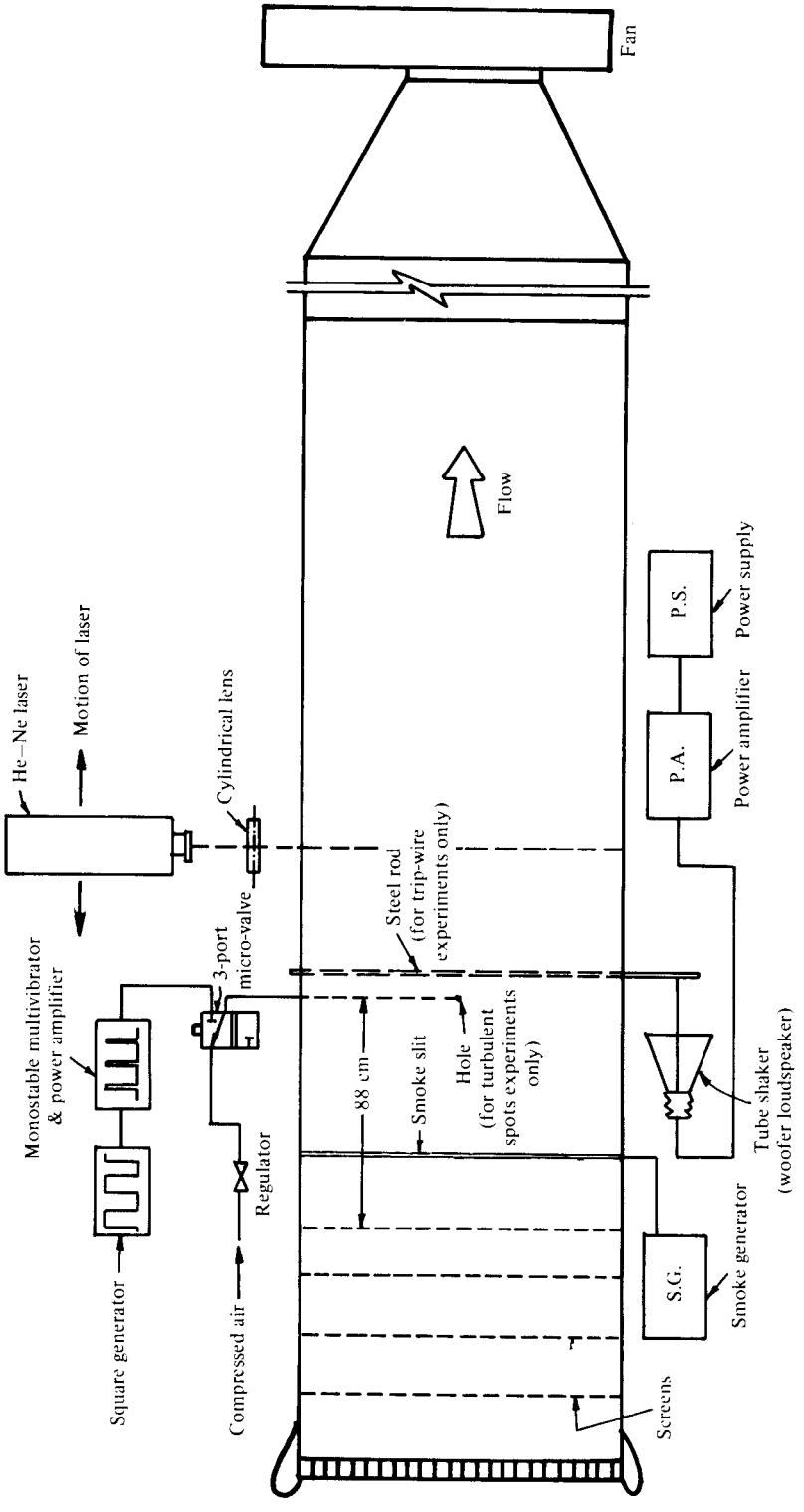

FIGURE 1. Layout of smoke tunnel and associated apparatus, plan view.

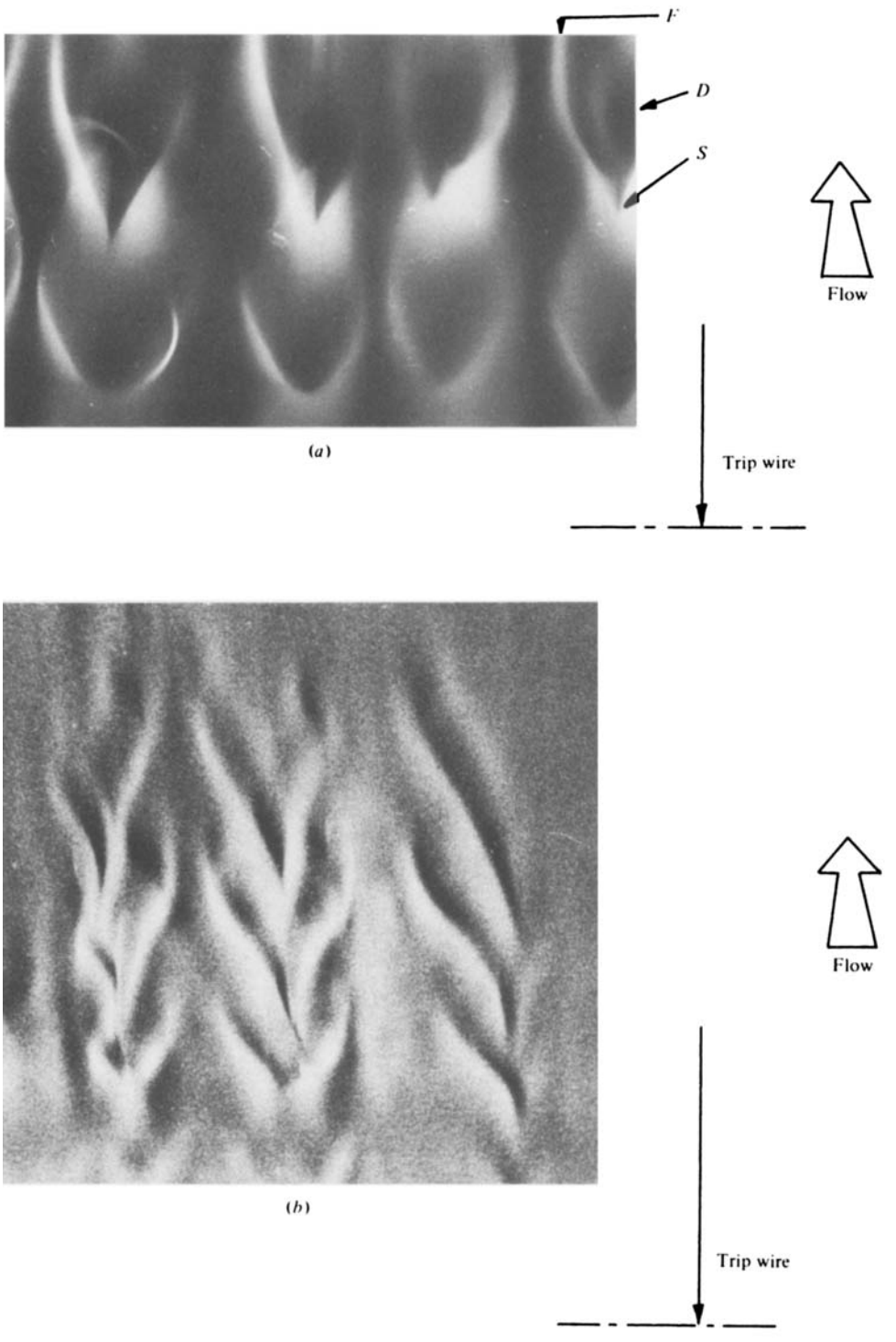

FIGURE 2. Typical smoke patterns showing the 'footprints' of the Λ-shaped vortices when the rod is above the smoke. (*a*) A close-up view of early stages. *S*, slit; *D*, depression; *F*, fold (definitions given in text). (*b*) A view further downstream. No forced oscillations were applied to the trip wire. $R_\delta^* = 160$; $R_x = 8700$.

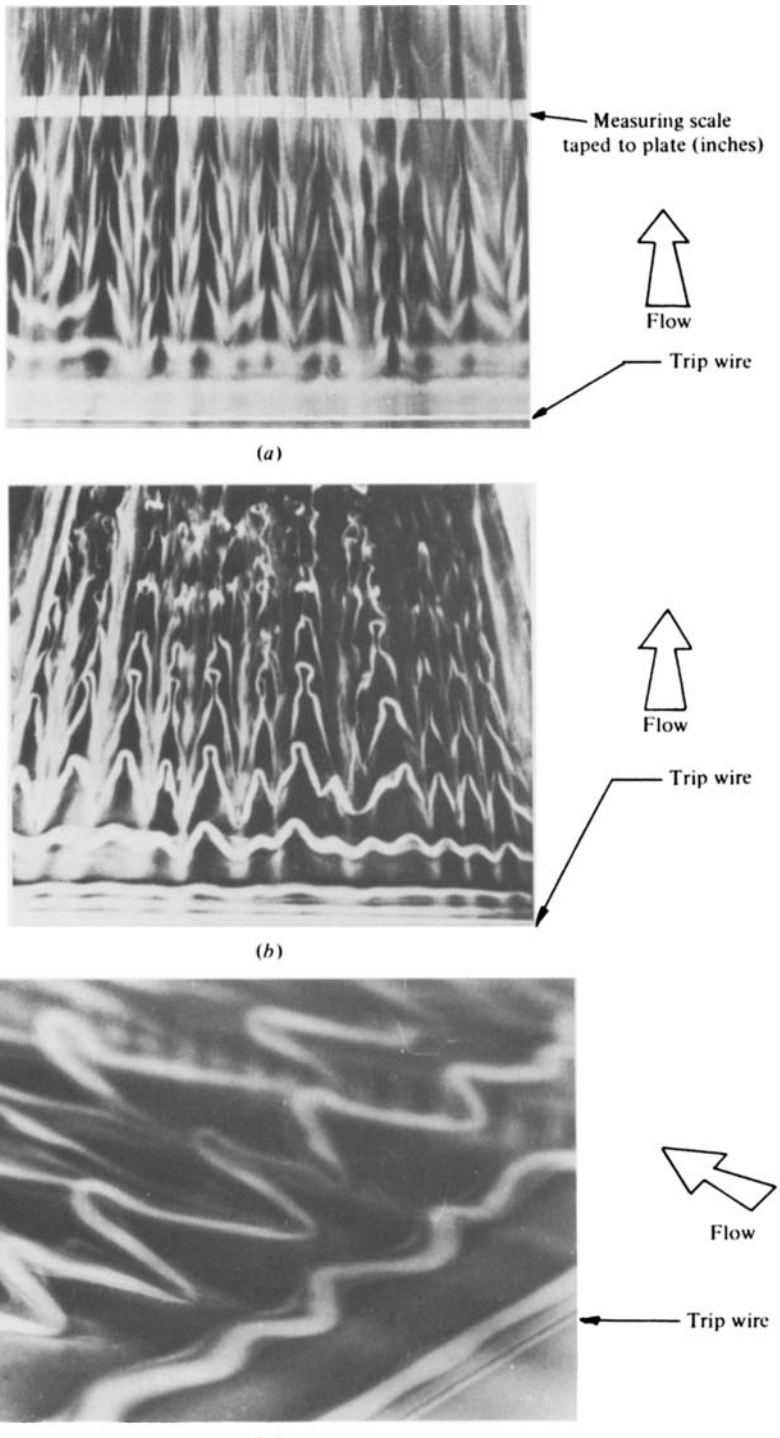

FIGURE 3. Typical smoke patterns of Λ-shaped vortices when the rod is submerged in the smoke. $R_\delta^* = 320$; $R_x = 34900$ for all cases shown here. (*a*) No forcing. (*b*) Forcing applied to wire. $\beta^* = 0{\cdot}297$; $f^* = 1{\cdot}47 \times 10^{-4}$. (*c*) An oblique of (*b*) above.

and Klebanoff, Tidstrom & Sargent (1962), who used vibrating ribbons. However, unlike the vibrating ribbon experiments, the rod was oscillated back and forth in a streamwise direction instead of up and down. The experimental arrangement for oscillating the trip wire is shown schematically in figure 1.

As a rough guide for adjusting the flow conditions for unstable behaviour of the laminar boundary layer, $U_1\delta^*/\nu$ ($=R_\delta^*$) was chosen to be of order 550 and

$$\beta\delta^*/U_1 = \beta^* = 0{\cdot}1,$$

where β is the frequency in rad/s. Here U_1 is the free-stream velocity and ν is the kinematic viscosity. This puts the operating point of the laminar layer in the unstable zone on the Tollmien plot of β^* *versus* R_δ^* (see Schlichting 1979). Thus, at a streamwise distance of 96 cm and a free-stream velocity U_1 of $1{\cdot}64\,\mathrm{m\,s^{-1}}$, this operating point is achieved giving a streamwise Reynolds number $R_x = 1{\cdot}02 \times 10^5$, and a non-dimensional frequency $f\nu/U_1^2 (= f^*) = 2{\cdot}86 \times 10^{-5}$, where f is the frequency in hertz. Under these conditions, the phase velocity and streamwise vortex spacing conformed closely with the calculated Tollmien values (phase velocity of $0{\cdot}6\,\mathrm{m\,s^{-1}}$ and a wavelength of approximately 11 cm). However, it should be remembered that the Tollmien stability criterion is based on a linear theory with two-dimensional waves. In the experimental situation, the disturbance would have been nonlinear. The rod diameter of 4·15 mm was not small compared with the boundary-layer thickness δ of 1–2 cm and, when forced, the amplitude of oscillation of the rod was not small, being 1–2 mm. Also, the authors found that one could operate outside the Tollmien instability zone and still produce the same type of patterns. In fact, the patterns for the trip wire shown in figures 2 and 3 were outside the stability zone. In these cases, the velocities were low and as a result thicker smoke patterns were produced which aided greatly in the photography. In the unforced situation these patterns sometimes decayed further downstream but this was never so when the rod was oscillated. The Reynolds number and non-dimensional forcing frequencies for the cases shown are quoted in the figure captions. For the forced patterns shown in figure 3 (*b*) and (*c*), the lateral spacing of the Λ-vortices was approximately 5·6 cm and the streamwise spacing was approximately 8 cm.

The photograph in figure 3 (*b*) shows quite clearly that the vortex filaments have a strong tendency to develop a three-dimensionality giving a longitudinal or streamwise component of vorticity. These vortex filaments initially develop a triangle-like wave form like a lot of interconnecting Λ's. These interconnecting Λ's possess both upstream and downstream apexes as defined in figure 4. Attempts were made to freeze these vortices by viewing them under stroboscopic light which was synchronized with the disturbing oscillation. The first four rows of vortices were frozen but further downstream randomness and disintegration of the structures made a detailed description difficult.

The lateral spacing of these Λ's does not appear to depend on the flow velocity or the trip-wire diameter. In fact, adding bands of adhesive tape at various spacings along the rod had little influence on the lateral spacing. Cellular flow present in the immediate wake of the rod appeared to be unrelated to the vortex spacing. These vortices appeared to leave the rod in a two-dimensional manner as can be clearly seen in figure 3 (*b*) and then rapidly developed a three-dimensional shape. It has been shown by Klebanoff &

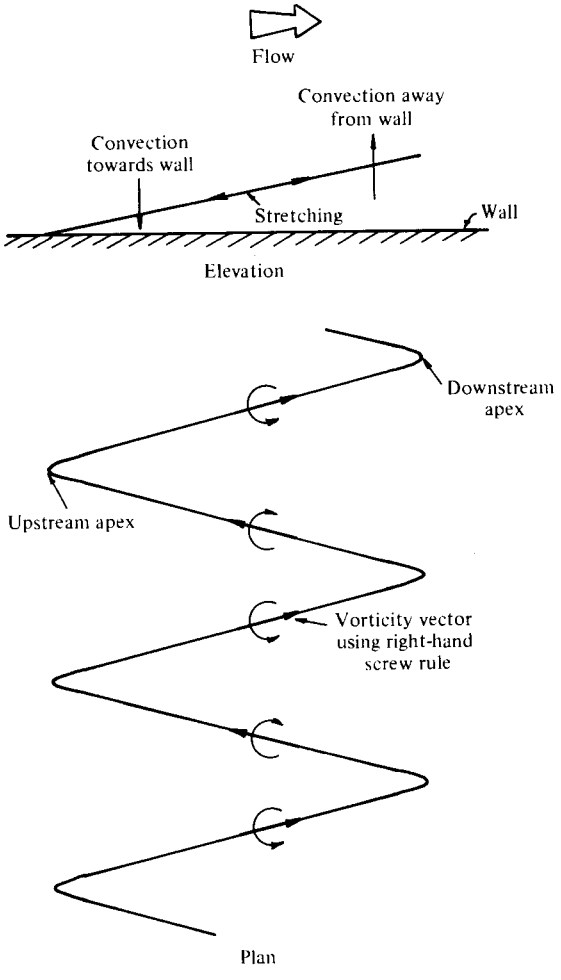

FIGURE 4. A schematic orthographic view showing the Λ-shaped vortices being stretched.

Tidstrom (1959) that irregularities in the wind tunnel screen system determine this lateral spacing. A cursory check was made by the present authors by replacing the last screen with a finer mesh and this *did* alter the vortex spacing. This, however, may not be a general result for all wind tunnels or flow conditions.

As mentioned by Hama & Nutant (1963), these bent vortex filaments tend to convect themselves towards the wall at the upstream apex and convect themselves away from the wall at the downstream apex. The Λ-shaped vortices stretch very rapidly as illustrated in figure 4 as they are convected downstream.

Klebanoff *et al.* (1962) pointed out that it is sometimes unjustified to assume that concentration of vorticity corresponds to the higher concentration of smoke. However, a laser cross-section shown in figure 5(*a*) illustrates clearly that the smoke shows a characteristic 'scroll' leading one to suspect a concentration of vorticity. Dr P. Klebanoff in a private communication questioned whether the smoke filaments in figure 3 were indeed vortex filaments. Strictly speaking, one should not refer to them

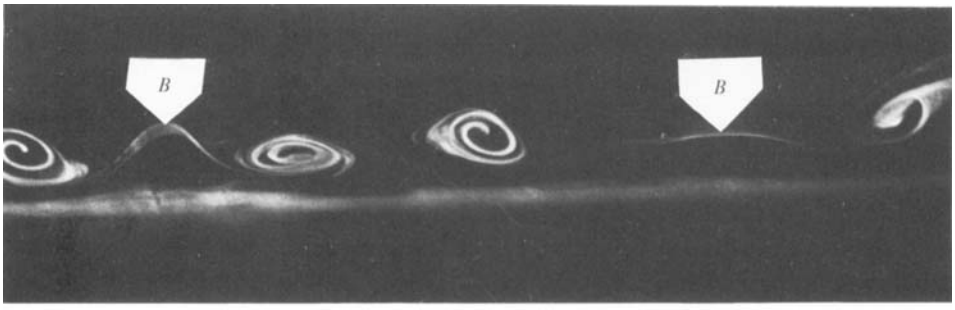

(*a*)

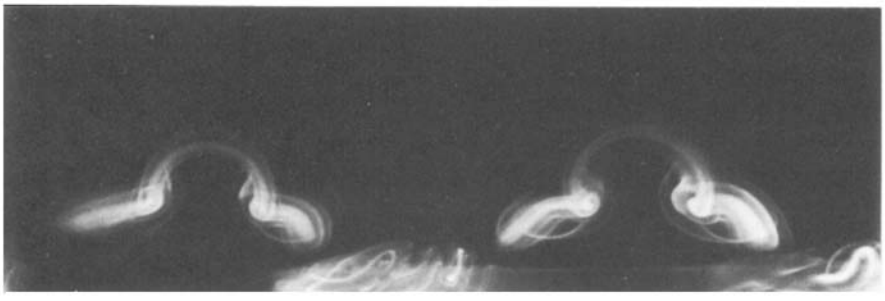

(*b*)

FIGURE 5. (*a*) Laser cross-section of smoke pattern behind rod submerged in the smoke. Sectioning is close to upstream apex. B is the bump as computed in figure 6(*d*). (*b*) End view with diffuse light looking upstream of a Λ-vortex with an Ω-shaped secondary vortex. For both cases $R_\delta^* = 320$; $R_x = 34900$, $\beta^* = 0{\cdot}297$, $f^* = 1{\cdot}47 \times 10^{-4}$.

as vortex filaments since vorticity is distributed spacially throughout the flow, but the authors contend that the smoke filaments are located at concentrations of vorticity. This was verified by placing a normal hot-wire in turn on either side of the legs of the Λ-vortices and viewing the vortices under stroboscopic light. A pulse from the strobe was displayed with the hot-wire signal and this revealed that, each time a smoke filament came near the wire, a sharp increase or decrease in velocity occurred at the wire depending on which side of the leg the wire was placed. This showed fairly conclusively that the smoke filaments did indeed consist of concentrations of vorticity and that the sign for the vorticity as assumed by the authors as shown in figure 4 was correct.

The secondary Λ-vortex which develops into an Ω shape as discussed by Klebanoff *et al.* (1962), Kovasznay, Komada & Vasudeva (1962) and Hama & Nutant (1963) is clearly visible in figure 5(*b*). See also figures 3(*b*) and 3(*c*). These authors pointed out that the extra Ω shape at the downstream apex of the Λ-vortex breaks down into a more complex form of instability further downstream. This, however, is not the authors' concern here. The main point the authors wish to emphasize is that, when Λ-shaped vortices occur, certain recognizable 'signatures' or 'footprints' are produced. As will be seen later, these signatures are also observed in turbulent spots.

A detailed description of these patterns will now be attempted. When the vortices are generated above the air–smoke interface, the upstream apex of the Λ's is convected towards the wall, is stretched longitudinally in the streamwise direction and gives the

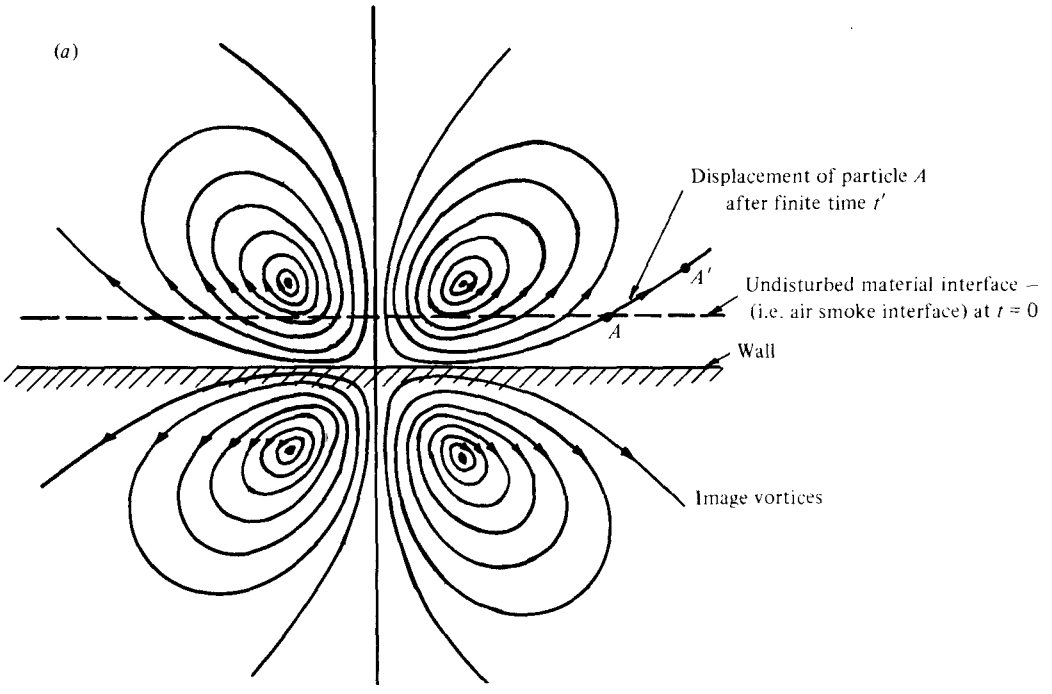

FIGURE 6 (*a*). For the caption see next page.

characteristic footprint patterns shown in figure 2 (*a*) and (*b*). An explanation of these patterns can be obtained from a very crude and simple mathematical model consisting of a trailing potential vortex pair with images. This was used to represent the downstream apex region as shown in figure 6 (*a*). Since the air–smoke interface has experienced the influence of the vortex filaments for a longer time as we move upstream, this distance upstream will be assumed to be 'time-like' for the purposes of calculating the deformation of the air–smoke interface. The displacement of the various points along the air–smoke interface were found by integrating their velocity along the streamlines shown in figure 6 (*a*) for various times. The results of these calculations are shown in figure 6 (*b*) and (*c*) for the case of vortex filaments above the undisturbed material interface. This gives a folded surface which resembles the patterns shown in figure 2. Figure 6 (*b*) also aids in defining various terms. The 'folds' are those parts of the deformed interface which are wrapped around the vortex filaments. The gap between the folds tapers to zero as we move further upstream, giving the appearance of a tapered slit when viewed from above. The folds themselves consist of smoke which has been elevated some distance above the initially undisturbed air–smoke interface. In figure 6 (*c*) it can be clearly seen that this elevated smoke has, immediately downstream of it, a depression where the level of smoke is below the initially undisturbed air–smoke interface. Folds are labelled F, depressions D and slits S. These same labels have been applied to the patterns shown in figure 2 (*a*).

For the case where the vortex filaments are below the initially undisturbed air–smoke interface, a different pattern emerges. This would occur if the rod was submerged in the smoke. Figure 6 (*d*) shows the calculated pattern and one can see that a

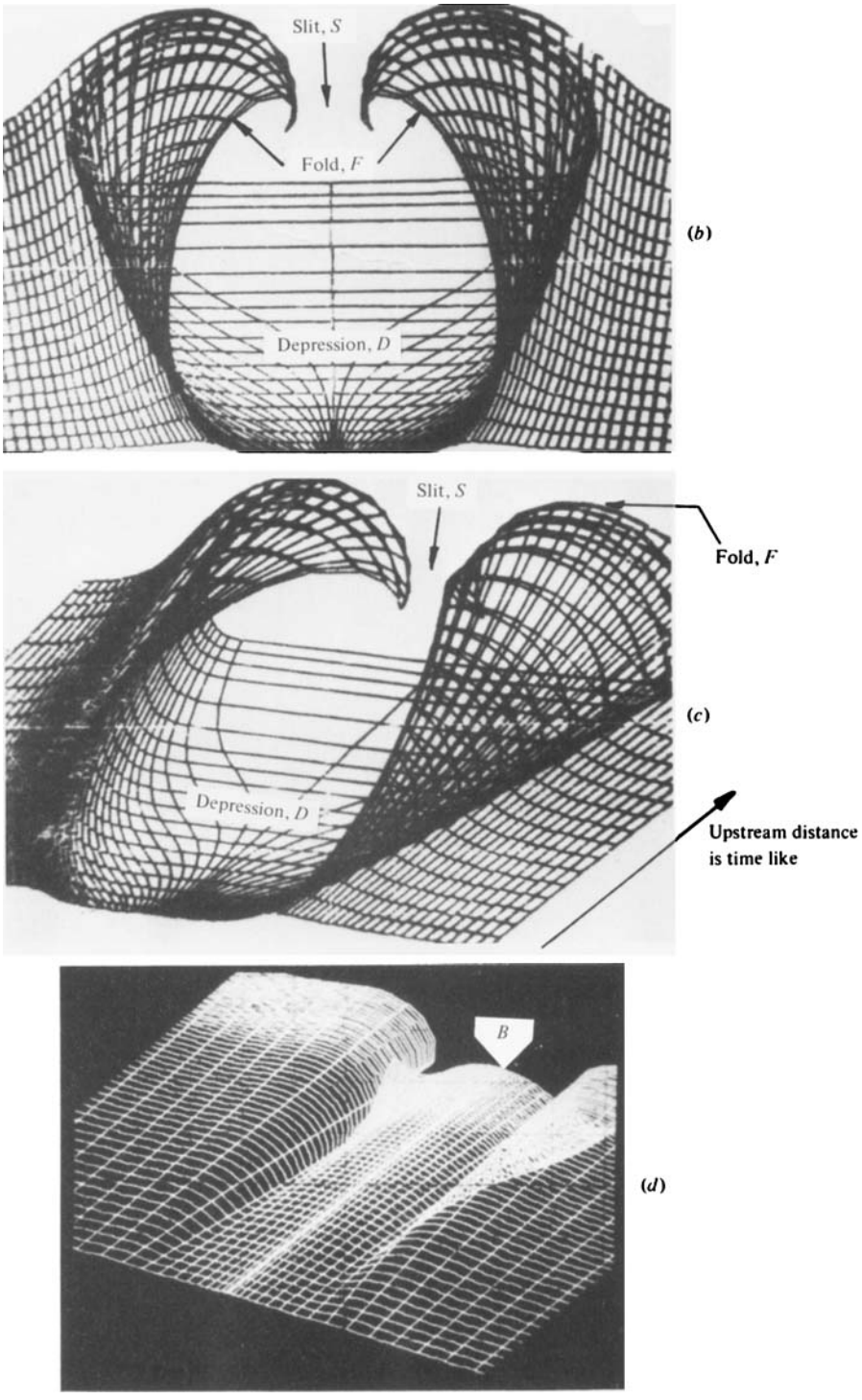

FIGURE 6. (*a*) Trailing vortex pair with images to simulate upstream apex of Λ-vortices. (*b*)–(*d*) Computer plots of a deformed material interface which may be identified with a deformed air–smoke interface. (*b*, *c*) The vortices were above the smoke interface. (*b*) View upstream but looking down at an angle to the plate. *S*, slit; *D*, depression; *F*, fold. (*c*) Isometric view. Distorted grid shown was initially a plane horizontal rectangular grid. (*d*) The vortices are below the smoke interface. Isometric view looking upstream. *B*, bump (see figure 5*a*).

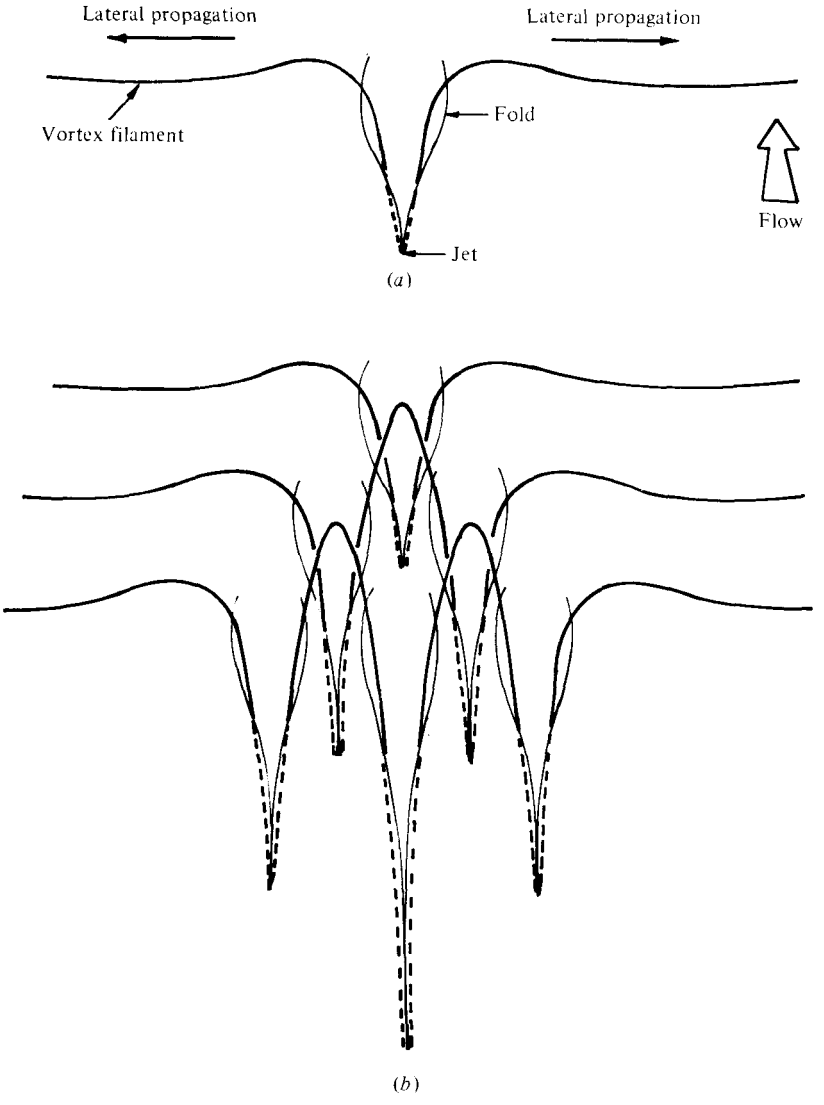

FIGURE 7 (*a*, *b*). For the caption see next page.

bump labelled *B* occurs. This resembles closely the pattern shown in figure 5 (*a*) where this bump is also labelled *B*. The Λ-vortex which appears in the experiments for this case does not appear in the calculations illustrated in figure 6 (*d*), since here only the upstream apex region is being modelled.

3.2. *Turbulent spots*

The trip wire in the tunnel was removed and a turbulent spot was initiated by a short pulse ($\simeq$ 20 ms) of air from a hole 3 mm in diameter drilled nornal to the tunnel floor 88 cm from the last screen. The pulse was made by sending a signal to an electromagnetic air microvalve which was connected to the air supply. The air pressure was increased until a spot just formed from a pulse. If the air pressure was too high, the

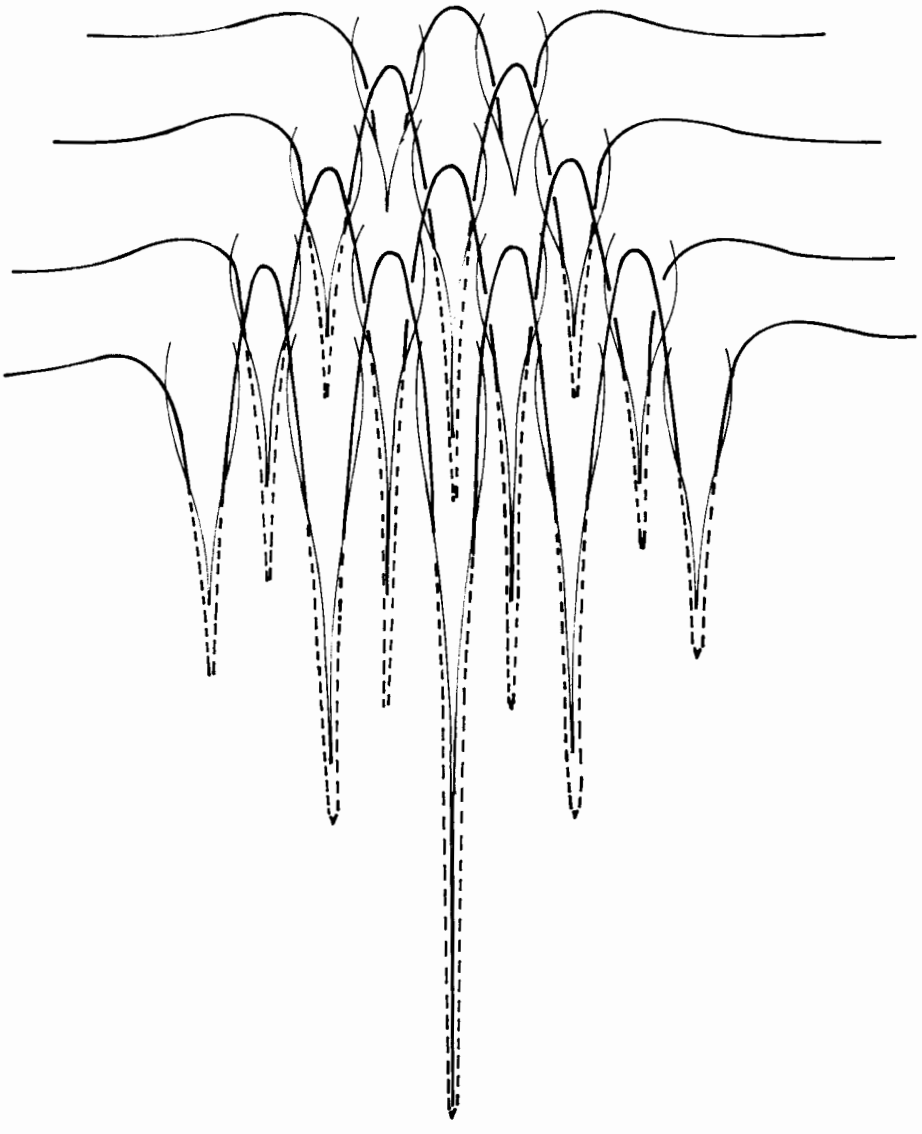

(*c*)

FIGURE 7. Schematic diagrams of the sequence of events leading to the formation of a turbulent spot in terms of vortex filaments. (*a*) A jet-initiated pulse caused the vortex filament to develop an undulation. (*b*) The initially disturbed filament has been stretched and developed two more undulations laterally. The filament in front has started to induced disturbances in the filaments further downstream. (*c*) The initially disturbed filament has developed two more undulations aterally.

nature of the spot would change in its initial stages but would look much the same as any other spot after a sufficient development. The experimental arrangement is shown schematically in figure 1. The most striking feature of the spot was that it possessed an array of folds on the wall which were very similar to those shown in figure 2. This led the authors to suspect that a turbulent spot consists of an array of Λ-shaped vortices.

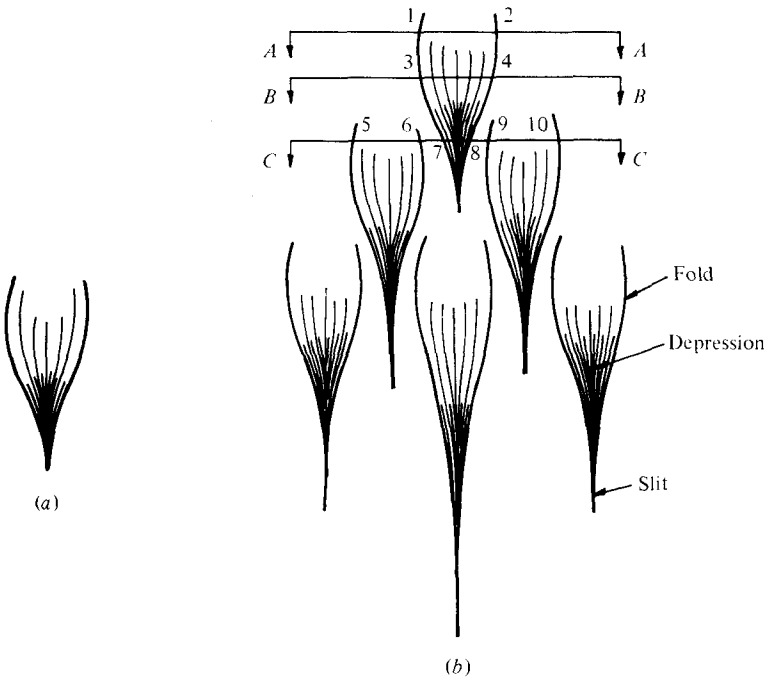

FIGURE 8 (*a*, *b*). For the caption see p. 401.

In fact, using this idea, one can explain five very important features of a turbulent spot, namely (1) the folds, (2) the staggered arrangement of these folds, (3) the long tapered tails which trail behind the spot, (4) the appearance of 'loop-like' structures after a sufficient development and (5) the characteristic heart-like shape of the spot.

Figures 7 (*a–c*) show schematic diagrams of the sequence of events which lead to the formation of a turbulent spot in terms of vortex filaments. The relationship of these filaments with the folds is also shown. Let the undisturbed laminar boundary layer be regarded as being made up of a field of straight cross-stream vortex filaments. Consider figure 7 (*a*). Here the jet has released a pulse and has caused a bundle of filaments to develop into a V-shaped vortex. The wavy line which is labelled as a vortex filament in figure 7 should actually be regarded as the 'centroid' of a bundle of these cross-stream filaments which wrap around each other to form a wavy 'rod' of vorticity near the disturbance. The authors conjecture that this disturbance shown in 7 (*a*) causes waviness in the vortex filaments to propagate laterally in the spanwise direction as shown. In figure 7 (*b*), this disturbance has been stretched and more undulations have formed in the original filaments. The undulations which point downstream induce a 'back-flow' in velocity beneath them, causing the undisturbed filaments ahead (downstream) to develop waves which are distributed in the spanwise direction 180° out of phase with those upstream. In figure 7 (*c*) the initially disturbed filaments, which have been stretched even more, have developed two more undulations laterally and the filaments in front have started to induce ahead of them disturbances in the filaments further downstream. Thus the spot is propagating itself forward by a domino-like mechanism and is growing laterally at the same time. The characteristic heart-like shape and long tapered tails of a spot will be seen in figure 8 (*c*). Figures 8 (*a–c*) show

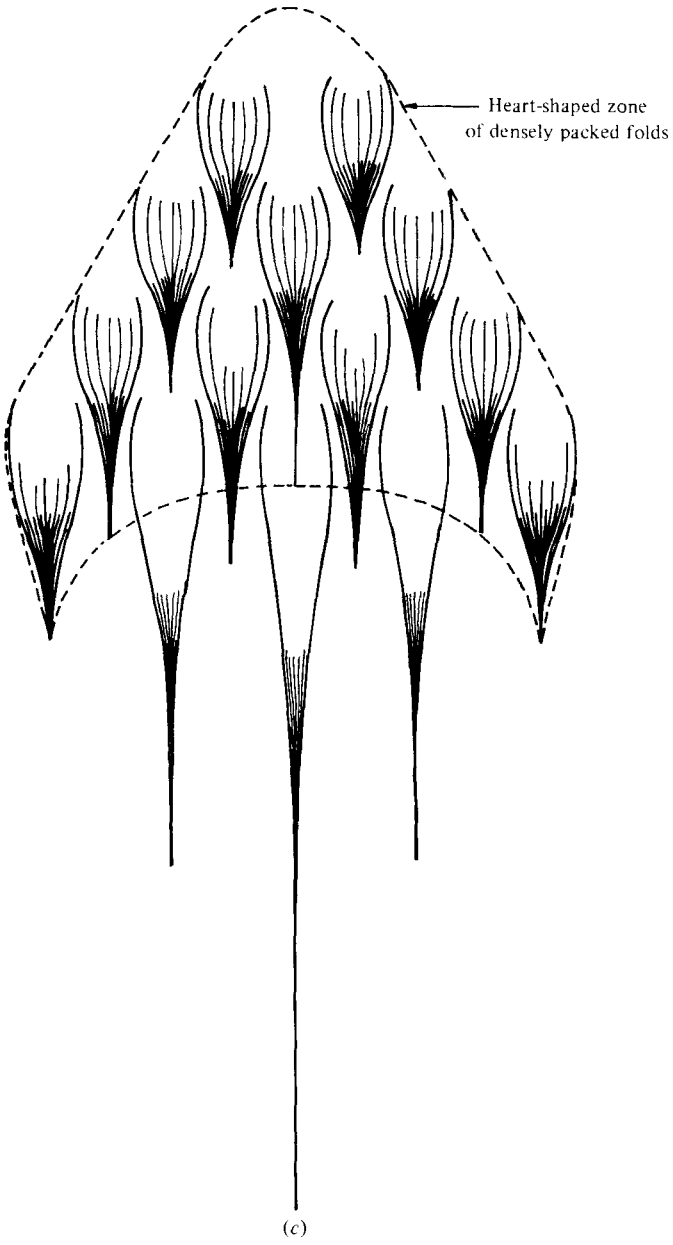

FIGURE 8 (*c*). For the caption see next page.

diagramatically the 'footprints' corresponding to figures 7 (*a–c*). Conjectured cross-sections are shown in figures 8 (*d*). As mentioned in the discussion regarding trip-wire patterns, there is a depression downstream of each fold with the characteristic slit and these are shown shaded in figure 8.

Figure 9 (*a*) shows a typical photograph of the 'footprints' of a turbulent spot produced in the surface of the smoke. The depressions, folds and slits can be seen and

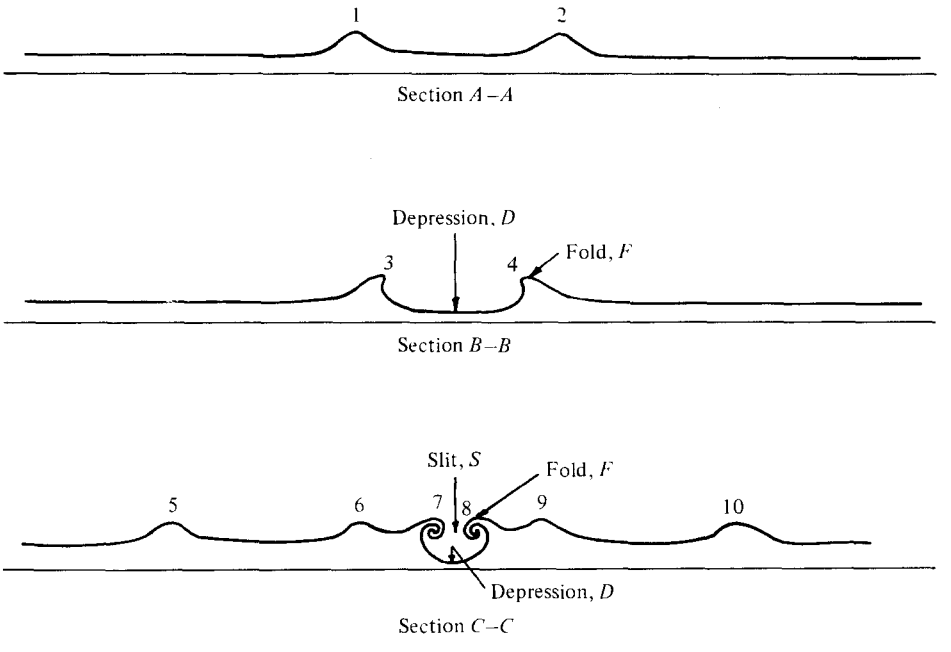

FIGURE 8. A sequence of 'footprints' corresponding to the arrangement of folds in figures 7(*a–c*). (*a*) A depression is shown shaded with the characteristic slit. (*b*) Two more folds are developed laterally corresponding with figure 8(*b*). (*c*) The depressions, folds and slits are shown to be arranged in a checker-board fashion inside an area heart-like in shape with long tapered tails. (*d*) Cross-sections. Numbers correspond to points shown in (*b*).

are arranged in a checker-board fashion inside a triangular or heart-like shaped area. The staggered nature of the arrangement of Λ-vortices is absent behind trip wires as can be seen in figures 2 and 3.

Figure 9(*b*) shows a more developed spot. Here sufficient entrainment of smoke from the wall has occurred and shows up as loop-like structures. When these structures first appear, they look like a jumbled-up version of the smoke patterns observed by Perry & Lim (1978) for positively buoyant wakes (see their figure 5*d* or their figure 3 inverted). Similar patterns can be seen in Cantwell *et al.* (1978) (see the longitudinal cross-sections given in their figures 7*a* for a spot and 7*b* for a boundary layer). However these patterns rapidly become very complex (probably because of instabilities as described by Hama & Nutant (1963) mentioned earlier). This complexity makes interpretations difficult. To the eye, these more developed structures look like the turbulent boundary-layer pictures of Bandyopadhyay & Head (1979) and the smoke photograph of Falco (1977).

Figure 9(*c*) shows a typical spanwise laser cross-section of a turbulent spot at an early stage of development. The patterns shown in figures 7 and 8 are of course very orderly, neat and simple, whereas the real case is somewhat disordered.

As indicated in figure 8(*c*) the authors believe that the tails of the turbulent spot are nothing more than the folds at the upstream end of the spot being stretched out over long streamwise distances. The folds at the centre are stretched more than those at the

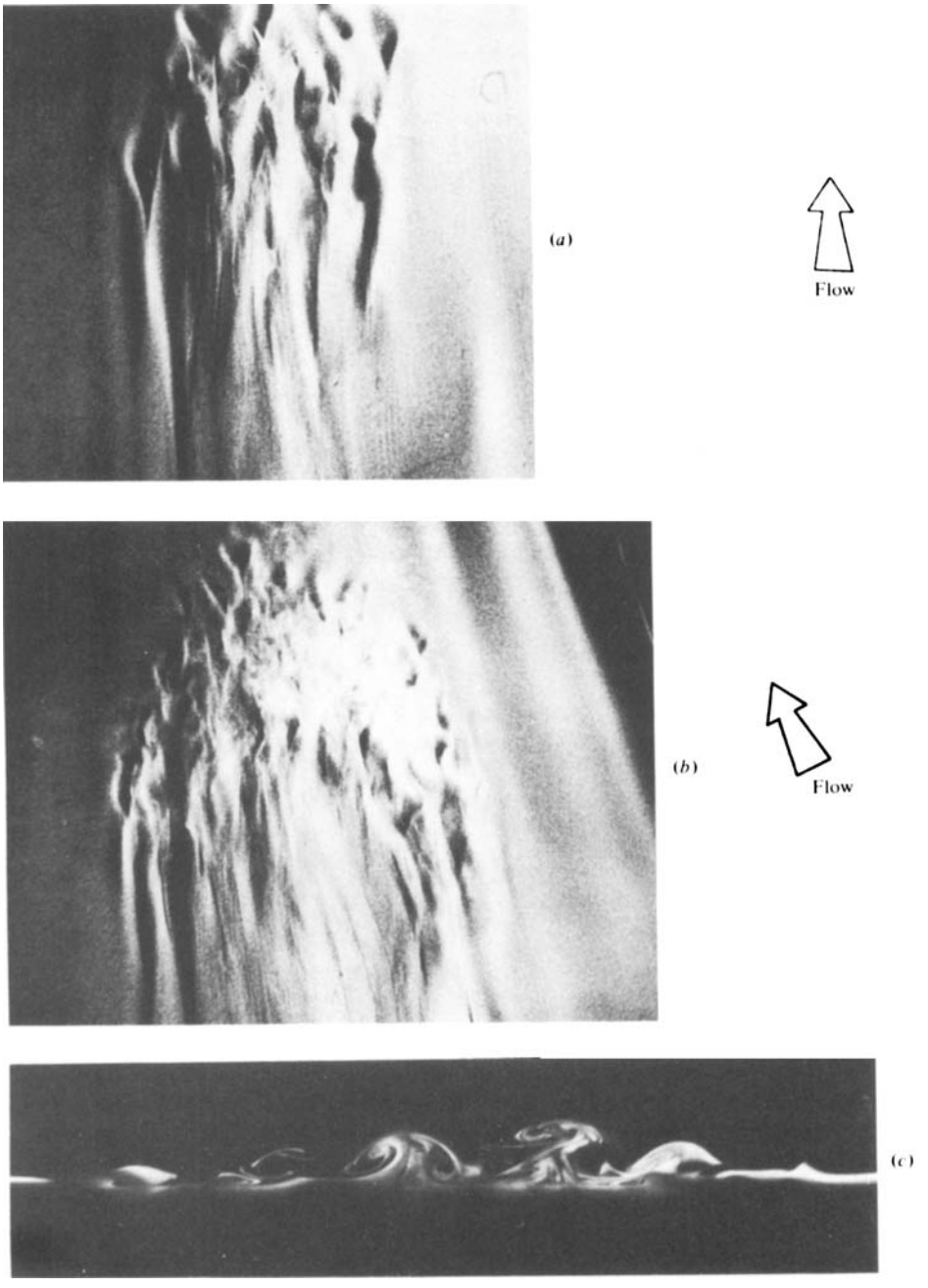

FIGURE 9. (*a*) Early stage of turbulent spot development. (*b*) A well-developed turbulent spot. (*c*) Laser cross-section of turbulent spot. For turbulent spot tests, R_δ^* varies from 307 to 431 (i.e. R_x varied from 32×10^3 to 57×10^3 at the point of initiation).

sides since they had formed earlier. This causes the triangular region of densely packed folds to appear heart-shaped.

The undulations which occur in the vortex filaments and the way the disturbances propagate laterally and forward bears a similarity to the wave-packet model of Gaster (1975) and Gaster & Grant (1975). However, the authors feel that nonlinearities would need to be included in this model if it is to predict the observations reported here. The predictions bear a resemblance with the streamwise behaviour but not with the spanwise behaviour.

The authors believe that the description given here, although simplified, gives the essential properties of a turbulent spot. However, other complex instabilities occur after a sufficient development of the spot. These instabilities appear to develop in the side tails of the spot and look something like the Perry & Lim (1978) patterns mentioned earlier. These might be connected with the instabilities noted by Wygnanski, Haritonidis & Kaplan (1979). These authors noticed very coherent wave packets which trailed after a fully turbulent spot. Another complex feature is that vortex loops at the upstream end of the heart tended to 'climb' over those further downstream. All of the above complexities have not been pursued in this present study. Unlike the case with the trip wire, the spanwise spacing of the Λ's in a spot is flow dependent and decreases with Reynolds number. The distance between adjacent upstream apexes is given by $\lambda \simeq 4{\cdot}9\delta^*$, where δ^* is the displacement thickness of the undisturbed laminar boundary layer measured at the jet. The spacing λ was measured 130 cm from the last screen and this spacing did not appear to vary significantly with subsequent downstream development. These tests were verified for a velocity range of 0·56–1·08 m s^{-1} giving a Reynolds number R_δ^* in the range of 316–439, at the point of initiation of the spot.

It has been conjectured by many workers that the central region of a turbulent spot should have the same structure as a fully turbulent boundary layer. One would therefore expect that the spacing λ of the longitudinal streaks should be given by

$$\frac{\lambda U_\tau}{\nu} = \lambda_+ = 100,$$

where U_τ is the friction velocity – for example see Kline (1967). From data given by Schlichting (1979) the local skin friction coefficient $C_f' \simeq 0{\cdot}005$ immediately after transition. In fact, this seems to be about the highest attainable skin friction on a smooth surface. Assuming that this is applicable to the spot, then, from the measured values of λ, this gives $\lambda_+ = 80$ for $U_1 = 0{\cdot}56$ m s^{-1} and $\lambda_+ = 105$ for $U_1 = 1$ m s^{-1}. Thus in view of the uncertainties of the measurements and calculations, this result is very encouraging and supports the connection between turbulent spots and turbulent boundary layers. In contrast to this, it appears unlikely that the structures which form immediately behind the trip wire have spacings which conform with $\lambda_+ = 100$. Presumably, one must regard these structures as 'unnatural' or 'synthetic'. However, as we go downstream, new Λ-vortices are probably generated which conform to the $\lambda_+ = 100$ scaling but are not visible. Such vortices could be thought of as belonging to an 'inner-flow' scaling whereas the vortices originating from the trip would belong to an 'outer-flow' scaling. Such scalings are suspected to occur in fully developed turbulent boundary layers.

4. Discussion and conclusion

The description of a turbulent spot as given here appears to be consistent with the five essential properties stated earlier. Attempts to obtain further verification by introducing smoke at elevated positions above the wall proved unproductive because of disturbances introduced by the apparatus. Although the authors' proposal appears simple, it seems very unlikely that hot-wire or laser-Doppler anemometry alone will verify this description.

What is really needed is an experiment in which identical spots can be produced by periodic disturbances thus enabling them to be frozen. Phase-averaged measurements with anemometers could then be utilized to obtain the detailed motions. Attempts to 'freeze' a spot so far have failed and any phase averaging would simply result in a big-eddying-type of description because of phase jitter and the associated washout of data.

The description given, namely an array of Λ-vortices, appears to be consistent with current models for the structure of fully developed turbulent boundary layers.

The authors wish to thank colleague Dr M. S. Chong for the mathematical computations. This project was financially supported by the Australian Research Grants Committee and the Australian Institute of Nuclear Science and Engineering. The authors also wish to acknowledge the very fruitful and stimulating discussions they had with Dr P. Klebanoff of the N.B.S., Washington, D.C.

REFERENCES

BANDYOPADHYAY, P. & HEAD, M. R. 1979 Film: Visual investigation of turbulent boundary structure. Engineering Department, University of Cambridge.

CANTWELL, B., COLES, C. & DIMOTAKIS, P. 1978 Structure and entrainment in the plane of symmetry of a turbulent spot. *J. Fluid Mech.* **87**, 641–672.

COLES, C. & BARKER, S. J. 1975 Some remarks on a synthetic turbulent boundary layer. In *Turbulent Mixing in Nonreactive and Reactive Flows* (ed. S. N. B. Murthy), pp. 285–292. Plenum.

EMMONS, H. W. 1951 The laminar-turbulent transition in a boundary layer. Part 1. *J. Aero. Sci.* **18**, 490–498.

FALCO, R. E. 1977 Coherent motions in the outer regions of turbulent boundary layers. *Phys. Fluids Suppl.* **20**, 124–132.

GASTER, M. 1975 A theoretical model of a wave packet in the boundary layer on a flat plate. *Proc. Roy. Soc.* A **347**, 271–289.

GASTER, M. & GRANT, I. 1975 An experimental investigation of the formation and development of a wave packet in a laminar boundary layer. *Proc. Roy. Soc.* A **347**, 253–269.

HAMA, F. R. & NUTANT, J. 1963 Detailed flow-field observations in the transition process in a thick boundary layer. *Proc.* 1963 *Heat Trans. & Fluid Mech. Inst.*, pp. 77–94. Stanford University Press.

KLEBANOFF, P. S. & TIDSTROM, K. D. 1959 Evolution of amplified waves leading to transition in a boundary layer with zero pressure gradient. *N.A.S.A. Tech. Note* no. D-195.

KLEBANOFF, P. S., TIDSTROM, K. D. & SARGENT, L. M. 1962 The three-dimensional nature of boundary-layer instability. *J. Fluid Mech.* **12**, 1–34.

KLINE, S. J. 1967 Observed structural features in turbulent and transitional boundary layers. *Fluid Mechanics of Internal Flow* (ed. G. Sovran), pp. 27–79. Elsevier.

KOVASZNAY, L. S. G., KOMODA, H. & VASUDEVA, B. R. 1962 Detailed flow field in transition. *Proc.* 1962 *Heat Trans. & Fluid Mech. Inst.*, pp. 1–26. Stanford University Press.

PERRY, A. E. & LIM, T. T. 1978 Coherent structures in coflowing jets and wakes. *J. Fluid Mech.* **88**, 451–463.

SCHLICHTING, H. 1979 *Boundary-Layer Theory*, 7th edn. McGraw-Hill.

SCHUBAUER, G. B. & KLEBANOFF, P. S. 1956 Contributions on the mechanics of boundary-layer transition. *N.A.C.A. Rep.* no. 1289.

SCHUBAUER, G. B. & SKRAMSTAD, H. K. 1948 Laminar boundary layer oscillations on a flat plate. *N.A.C.A. Rep.* no. 909.

THEODORSEN, T. 1955 The structure of turbulenc 50 *Jahre Grenzschichtforschung* (ed. H. Görtler & W. Tollmien), p. 55. Braunschweig: Veiweg and Sohn.

WYGNANSKI, I., HARITONIDIS, J. H. & KAPLAN, R. E. 1979 On a Tollmien-wave packet produced by a turbulent spot. *J. Fluid Mech.* **92**, 505–528.

WYGNANSKI, I., SOKOLOV, N. & FRIEDMAN, D. 1976 On the turbulent 'spot' in laminar boundary layer. *J. Fluid Mech.* **87**, 641–672.